NANO LETTERS

LETTER

pubs.acs.org/NanoLett

Gallium Nitride Based Logpile Photonic Crystals

Ganapathi Subramania,*[,†,‡] Qiming Li,[†] Yun-Ju Lee,[§] Jeffrey J. Figiel,[†] George T. Wang,[†] and Arthur J. Fischer[†]

[†]Sandia National Laboratories, P.O. Box 5800, Albuquerque, New Mexico 87185, United States

[‡]Department of Electrical and Computer Engineering, University of New Mexico, Albuquerque, New Mexico 87131, United States

[§]Department of Materials Science and Engineering, University of Texas at Dallas, 800 West Campbell Road, RL 10, Richardson, Texas 75080, United States

Supporting Information

ABSTRACT: We demonstrate a nine-layer logpile three-dimensional photonic crystal (3DPC) composed of single crystalline gallium nitride (GaN) nanorods, ~100 nm in size with lattice constants of 260, 280, and 300 nm with photonic band gap in the visible region. This unique GaN structure is created through a combined approach of a layer-by-layer template fabrication technique and selective metal organic chemical vapor deposition (MOCVD). These GaN 3DPC exhibit a stacking direction band gap characterized by strong optical reflectance between 380 and 500 nm. By introducing a "line-defect" cavity in the fifth (middle) layer of the 3DPC, a localized transmission mode with a quality factor of 25−30 is also observed within the photonic band gap. The realization of a group III nitride 3DPC with uniform features and a band gap at wavelengths in the visible region is an important step toward realizing complete control of the electromagnetic environment for group III nitride based optoelectronic devices.

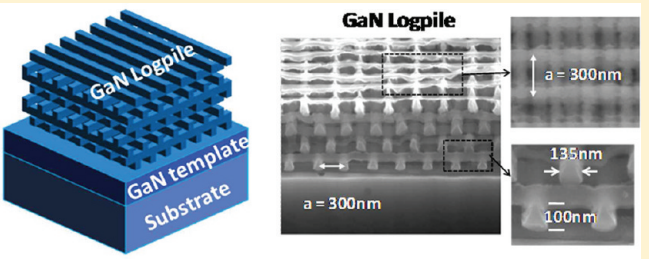

KEYWORDS: Three-dimensional photonic crystal, nanophotonics, gallium nitride, logpile, Electron Beam Lithography

Photonic crystals (PC) are artificial structures comprised of alternate regions of high and low refractive index materials in one, two, or three dimensions (3D) that can have a frequency gap or a photonic band gap where electromagnetic modes are forbidden. In a 3DPC with a suitable geometry and material composition, one can obtain a 3D photonic band gap where electromagnetic modes in all three dimensions are suppressed creating an electromagnetic vacuum.[1,2] This property of 3DPCs opens up new regimes of photon manipulation and light−matter interaction.

Herein, we focus on group III nitride based 3DPCs because group III nitrides are important semiconductors currently used or being explored for use in light-emitting diodes, laser diodes, photodetectors, and photovoltaic devices. Integrating 3DPCs with group III nitride devices will enable new strategies for enhancing the device performance. Inside a photonic band gap all radiative emission is suppressed while outside the gap one can obtain enhanced emission due to the increased photonic density of states.[1,3] 3DPCs can thus make radiative processes preferable to other undesired radiative and nonradiative processes by suitably modifying the electromagnetic environment surrounding the emitter. For example, control of light emission has been previously demonstrated by embedding nano light sources such as quantum dots[4−7] inside 3DPCs. Control of spontaneous emission would be particularly useful for enhancing the performance of LEDs especially at wavelengths in the green, yellow, and red where efficiency is particularly low. Thus far most efforts involving group III nitrides have focused on two-dimensional photonic crystals (2DPCs) as they are easier to fabricate. For example, group III nitride based 2DPCs have been utilized to improve light extraction efficiencies[8−12] and achieve highly directional emission.[13−16] 2DPCs typically offer light control along one plane but do not offer complete three-dimensional light control which is possible using 3DPCs. To date, a true 3DPC composed entirely of group III nitride has not been demonstrated to our knowledge.

In this paper, we demonstrate a nine-layer logpile 3DPC composed of single crystalline GaN nanorods, with lattice constants (a) of 260, 280, and 300 nm. The widths of the GaN nanorods are 100−135 nm which corresponds to 0.4a−0.45a. This unique GaN structure is created through a combined approach of a layer-by-layer template fabrication technique and selective metal organic chemical vapor deposition (MOCVD). This GaN 3DPC exhibits a stacking direction band gap characterized by a strong reflectance between 380 and 500 nm. The realization of a group III nitride 3DPC with uniform features and a band gap at wavelengths in the visible is an important step toward realizing complete control of the

Received: June 1, 2011
Revised: September 19, 2011
Published: October 04, 2011

ACS Publications © 2011 American Chemical Society

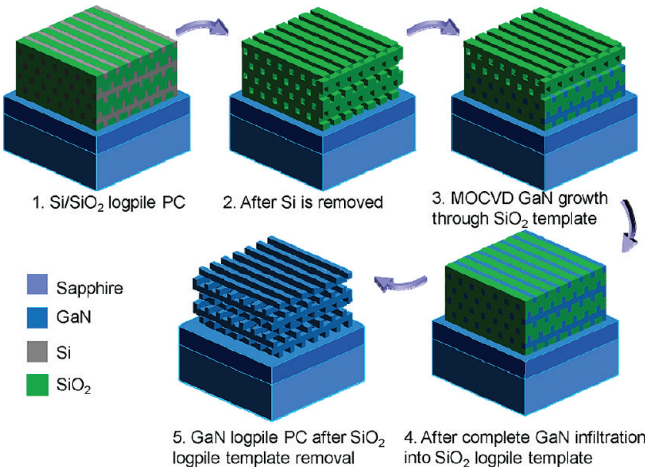
1. Si/SiO2 logpile PC
2. After Si is removed
3. MOCVD GaN growth through SiO2 template
4. After complete GaN infiltration into SiO2 logpile template
5. GaN logpile PC after SiO2 logpile template removal
Sapphire
GaN
Si
SiO2

Figure 1. Schematic of the fabrication of a GaN logpile from a template of a Si/SiO_2 logpile. Each layer was patterned using electron beam direct write.

electromagnetic environment for group III nitride based optoelectronic devices.

Fabrication of 3DPCs that can operate in the visible region has been challenging due to the submicrometer periodicity and features sizes involved as well as limited availability of high refractive index materials. Early approaches to visible 3DPCs were based on self-assembly of submicrometer spheres,[17−19] which resulted in numerous unintentional defects in these PCs making them unsuitable for device fabrication. A lithographic approach enables the fabrication of high-quality 3DPCs as demonstrated by TiO_2 based visible logpile 3DPCs.[20,21] In this approach each layer is patterned in a resist using electron beam lithography, which is then transferred to the underlying material (e.g., TiO_2) via dry etch using the resist as a mask. This approach cannot be directly applied to the fabrication of GaN based 3DPCs because of a lack of simple low temperature deposition methods for GaN as well as GaN's strong resistance to dry chemical etching. We overcome these problems by using a templated growth approach where GaN is introduced epitaxially into an inverted template of a logpile PC composed of SiO_2. Our approach is based on a previous demonstration of metal organic chemical vapor deposition (MOCVD) GaN growth through a silica microsphere template which was done for the purpose of reducing the dislocation density.[22]

For our growth process we start with 2-in. *c*-plane sapphire wafers with a ~2 μm thick GaN epitaxial layer that acts as a seeding layer for subsequent GaN PC growth. A schematic of the process is shown in Figure 1. We first fabricate a logpile PC composed of Si/SiO_2 using a multilevel electron beam direct write approach.[20] When the samples are immersed in an aqueous KOH solution (20 wt %) at room temperature, the silicon is selectively removed to leave behind a SiO_2 logpile. The logpile PC consists of a continuous network of connected voids that provides a path for transport of the metal organic precusors to the bottom GaN seeding layer. During the GaN logpile growth, typical conditions for growing planar GaN lead to a 3D growth mode inside the SiO_2 logpiles. During the 3D growth mode, GaN islands with a wide distribution in height form on the seeding layer. When these GaN islands reach the top surface of the SiO_2 logpiles, this surface is too rough to coalesce into a planar thin film, resulting in a structure with large pores (Figure 2a).

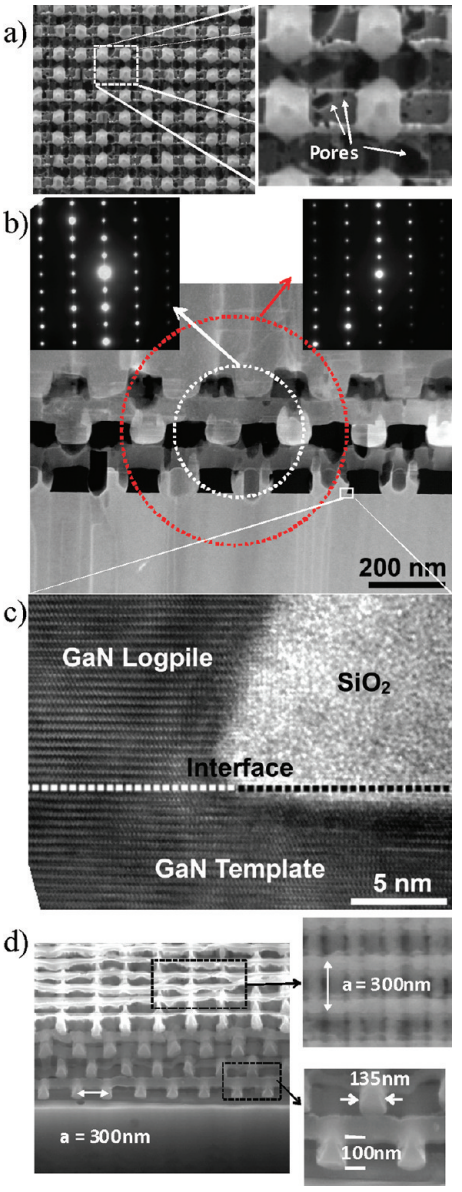

Figure 2. (a) SEM image of GaN logpile without optimal growth conditions showing large pores resulting from the 3D growth mode. (b) Cross-section TEM image of a five layer GaN logpile structure. Inset on the right-hand side shows an electron diffraction pattern from the region indicated by the dotted red circle and the left-hand side inset shows the diffraction pattern from the white dotted circle region. (c) HRTEM image of the region indicated by the white rectangle in (b) showing the growth of GaN at the interface between the SiO_2 logpile template and the bottom GaN template epitaxial layer. (d) Cross-section SEM image of a nine layer GaN logpile with a 300 nm lattice constant and rod height of 100 nm at lower pressure optimal growth conditions to enable nucleation on the GaN epilayer resulting in a 2D growth mode. The top right-hand side image shows an enlarged top view and the bottom image shows an enlarged section of the perspective view of regions indicated by dotted black box. The width of the rod is approximately 135 nm.

Therefore, we developed a special growth technique to promote a uniform two-dimensional growth mode. We found that reducing the growth pressure is the most efficient for achieveing 2D growth in the SiO_2 logpiles. This growth condition involves flowing 100 sccm of H_2 gas through a trimethylgallium (TMGa)

dx.doi.org/10.1021/nl201867v |*Nano Lett.* 2011, 11, 4591–4596

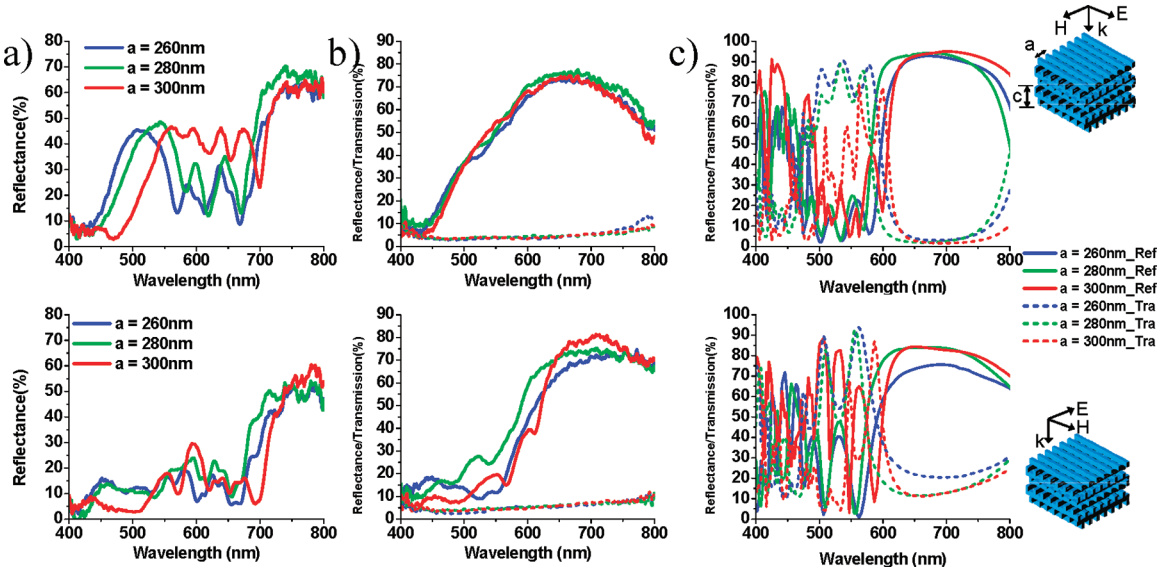

Figure 3. Optical reflectance spectrum in the visible region for a nine layer GaN logpile for input polarization parallel (top) and perpendicular (bottom) to the top layer rods. (a) Reflectance response with SiO_2 background still in place. (b) Reflectance (solid) and transmission (dotted) response after the SiO_2 has been removed showing a band gap in the visible region. (c) Finite difference time domain (FDTD) simulation response of the modeled logpile structure without the background SiO_2.

bubbler held at −5 °C with the NH_3 flow rate maintained at 4 SLM. The GaN was grown at a temperature of ∼1050 °C with the growth pressure ranging from 7 to 30 Torr using both H_2 and N_2 as carrier gases. Under these conditions, GaN selectively grows through the SiO_2 logpile template at a growth rate of approximately 1 μm per hour.

Figure 2b shows a cross-sectional *z*-contrast scanning transmission electron micrograph (TEM) image of GaN grown through a five layer SiO_2 logpile template. The GaN growth is continued after the logpile growth was completed to coalesce a ∼2 μm thick GaN layer over the GaN logpile. The electron diffraction pattern as shown in the top left inset in Figure 2b was acquried selectively from a small logpile region (indicated by the white dotted circle) and shows a single set pattern, indicating the single crystalline nature of the GaN logpile region. The lattice spacing extracted from the electron diffraction pattern matches the lattice constant of a *c*-plane GaN (5.178 Å) and *m*-plane GaN (3.189 Å). An electron diffraction pattern (top right inset) was also collected from a larger region (indicated by the dashed red circle) including the bottom GaN seeding layer, the logpile, and the top coalesced region. This reveals a pattern identical to that from the logpile region indicating that the GaN logpile grows homoepitaxially on the underlayering GaN seeding layer. To further confirm the homepitaxial reslationship, high-resolution TEM images were taken at the interfacial region between the GaN logpile, the GaN seeding layer, and the SiO_2 logpile templates, as highlighted by the white square in Figure 2b. The corresponding high-resolution TEM (HRTEM) image (Figure 2c) shows that the GaN logpile lattice aligns very well with the GaN templates with no sign of grain boundaries. Figure 2b also reveals small pores with two salient features: (1) the pores only appear near the interface between Ga-polar *c*-plane GaN logpiles and SiO_2 and (2) the pores show hexagonal facets as also seen in the plan view SEM image in Figure 2a. These features suggest that anisotropic thermal decomposition under a growth condition involving high temperature and H_2 leads to pore formation such that pores are not the result of defects in the SiO_2 logpile template.

Using a similar approach, we also grew another GaN logpile sample through a nine layer SiO_2 template. In this case we did not overgrow the GaN layer in order to have access for selective dissolution of the SiO_2 template. The SiO_2 was removed using 6:1 buffered oxide etchant, leaving behind a high index contrast ratio GaN/air logpile PC for subsequent optical measurements. Figure 2d shows scanning electron microscope (SEM) images of a tilted cross-section view image of a GaN logpile with a lattice constant of 300 nm after the SiO_2 is removed. The SEM image shows that the GaN logpile nanorods have formed with excellent alignment between the successive layers. The images on the right show an enlarged view of the top surface and the perspective is indicated by the black dotted box. The topmost (ninth) layer appears thinner than the other layers because the growth process was terminated before sufficient thickness was achieved. This problem can be addressed for future structures by further optimizing the growth time.

We fabricated logpile PCs with lattice constants of a = 300 nm, a = 280 nm, and a = 260 nm. To characterize the photonic band gap of the logpile structure[20,21] we performed optical measurements between 400 and 800 nm using a polarized light source that also enabled the measurement of the polarization dependence of the spectra on the orientation of the terminating layer.[21,23] Before the SiO_2 template is removed, for both input light polarizations, the reflectance spectra (Figure 3a) shows broad peaks emerging near 680−700 nm that extends toward longer wavelengths together with oscillations at shorter wavelengths. The rising edges of the broad peaks correspond to the upper band edge along the stacking directions while the oscillations correspond to higher band features of the GaN lopgile before template removal. For all three lattice constants, the parallel polarization case shows a maximum reflectance value of ∼70% and the perpendicular polarization ∼60%. The band edge for the a = 260 and 280 nm also show a blue shift of 20 nm

dx.doi.org/10.1021/nl201867v |*Nano Lett.* 2011, 11, 4591–4596

compared to the a = 300 nm case. Upon removal of the template, the reflectance response for both polarizations (Figure 3b solid curves) shows a considerable blue shift, which is expected since template removal reduces the effective refractive index of the entire PC. The reflectance spectra for the parallel polarization show a broad peak corresponding to the stacking band gap, spanning across the measurement region with a maximum reflectance of 75% while perpendicular polarization spectra show an upper band edge near 550 nm followed by a sharp rise to about 70−80% reflectance. The transmission response (Figure 3b dashed curves) reveals low transmission (<10%) for both polarizations. The reflectivity values measured are somewhat lower than that expected based on previous measurements made on visible logpile PCs fabricated from TiO_2[21] which has a refractive index similar to GaN.

To explore this further we performed a finite difference time domain (FDTD[24]) simulation of a nine layer GaN logpile without the SiO_2 background assuming a rod width ~0.4a−0.45a (based on SEM image measurement) and a nominal height for each layer of ~100 nm which was determined by measuring the template thickness for each layer. The simulations revealed two interesting aspects. First, the simulated spectra (Figure 3c) show very little spectral shift between the three different lattice constants for both polarizations as observed in the experimental spectra. The lack of the expected proportional shift in the spectra with lattice constant can be attributed to a difference in the ratios of vertical to horizontal lattice constants (c/a) (Figure 3a logpile cartoon) between the three different lattice constant devices. This occurs because the rod heights cannot be proportional to the lattice constants when fabricated on the same substrate.[25] Second, the simulated reflectance magnitude is somewhat higher than that observed in the experiment. For the parallel and perpendicular polarizations we obtain ~90% and 75−83% for the simulated spectra compared to ~75% and 70−80% for the experimental spectra, respectively. There is a ±5% variation in the measured value of reflectance and transmission arising from the difference in the location of the measurement spot on the device as well as errors arising from focusing of the microscope objective used for microspectroscopy. Some discrepancy is expected, as the microscope objective cannot collect all the beams including diffracted ones as can be done theoretically with FDTD using periodic boundary conditions. Additionally, the simulated reflectance spectra show higher order peaks not observed in the experiment. This difference is also apparent when comparing the transmission response for both polarizations with the simulated spectra. Since the cross-section TEM measurement reveals single crystalline GaN, these differences are unlikely to be due to absorption as the wavelengths are well below the absorption edge of GaN. These observed differences in magnitude and shorter wavelength features between the experimental and FDTD simulated spectra can be attributed to scattering behavior arising from any or a combination of the following reasons: (1) As seen from the SEM image (Figure 1b), the top layer is not fully formed and exhibits roughness which can significantly affect the coupling of incoming light and reduce reflectance and transmission due to scattering. (2) The small pores at the GaN/SiO_2 interface described earlier in Figure 2b could also be a source of scattering. (3) The GaN logpile layers are under compressive stress which, after the removal of the template, might lead to warping and internal cracking during stress release. This can potentially be minimized by introducing stress release trenches using focused ion beam (FIB) etching and/or further optimizing the growth. (4) GaN naturally grows with hexagonal symmetry while the logpile has square symmetry which can lead to roughness on either of the logpile rods depending on the orientation of the rods to the underlying epitaxial seeding layer. These nonidealities can be potential sources of scattering that can significantly affect the higher order peaks in addition to the reflectance/transmission magnitudes. Further optimization of epitaxial growth will be required to improve the optical response for future structures.

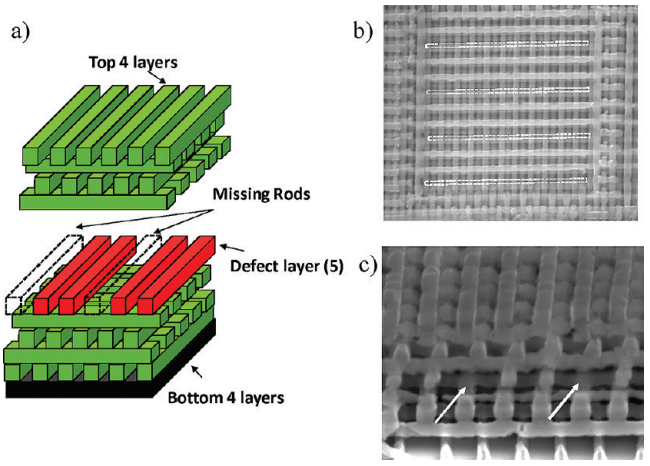

Figure 4. (a) A schematic view of a cavity defect introduced in the fifth layer (shown in red) consisting of missing rods (indicated by dotted lines). (b) Top view SEM image of layer five of the logpile obtained through a partial, focused ion beam (FIB) cut depicting a line defect cavity where every third horizontal rod has been removed. The missing rods are indicated by white dashed stripes. (c) Cross-sectional SEM image of the cavity structures. The white arrows point to the position of the missing rods.

Thus, SEM and TEM images combined with the optical response described above clearly indicate that it is possible to achieve a GaN based logpile photonic crystal with a band gap in the visible region by using the above procedure. Also, the optical quality of the GaN logpile is comparable to planar epitaxial GaN, as seen from the photoluminescence response where both indicate similar yellow luminescence (see supplemental figure in the Supporting Information). This demonstration is a crucial step toward GaN 3DPC based solid state lighting devices. 3DPCs, particularly logpile structures with the potential for a full 3D gap, can dramatically enhance light emission by enhancing the photonic density of states (PDOS) at the photonic band edge. Another approach to enhancing the PDOS is by utilizing cavity modes created within the photonic band gap by breaking the periodicity of the PC through intentional defects.

To demonstrate this we fabricated a "line-defect cavity" by periodically removing an entire rod in the fifth layer of our nine layer logpile structure. Figure 4a shows a schematic of the cavity structure while panels b and c of Figure 4 show the top view and cross-sectional SEM image, respectively, of such a cavity where every third rod is removed. The optical reflectance measurements show that the response of the cavity to the input light is highly polarization dependent (Figure 5a). Thus for light polarized parallel to the fifth layer rods, we observe a reflectance dip within the band gap appearing at wavelengths of 730 nm for a = 300 nm, at 695 nm for a = 280 nm, and at 685 nm for a = 260 nm structures. This indicates that we can achieve frequency tunability

dx.doi.org/10.1021/nl201867v |*Nano Lett.* 2011, 11, 4591–4596

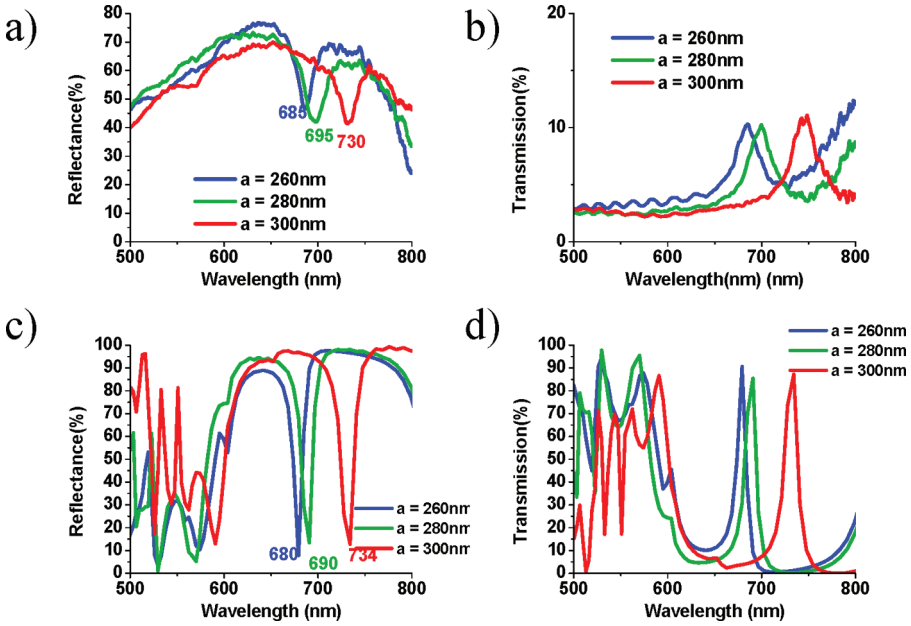

Figure 5. (a) Optical reflectance spectrum of the line-defect cavity structures. Dips in the reflectance corresponding to the cavity mode appear at 730, 695, and 685 nm for a = 300, 280, and 260 nm, respectively. (b) Corresponding transmission spectrum. (c) FDTD simulation of the reflectance spectrum of the cavity structures. (d) Simulation of the corresponding transmission spectrum.

of the cavity modes by changing the lattice constant of the photonic crystal. Figure 5b shows the corresponding transmission response which clearly indicates that transmission modes within the band gap are opened up by the cavity. The measured quality factors (Q) are similar for each lattice constant with values of ~28, 26, and 29 for a = 260, 280, and 300 nm, respectively. FDTD simulation of the structure also shows reflectance dips/transmission peaks (Figure 5c,d) associated with the cavity modes. The simulated reflectance dips (Figure 5c) match the experimental ones quite closely in wavelength however they are considerably deeper than the measured dip. Since quality factor (Q) is defined as $\lambda_{dip}/\Delta\lambda$, where $\Delta\lambda$ is the full width at half-maximum (fwhm), the deeper the reflectance dip, the smaller the fwhm which results in a larger Q. As such, the calculated quality factors in Figure 5c have values of ~68, 46, and 43 for a = 260, 280, and 300 nm, respectively, which is larger than the experimental values. The previously discussed explanation for the discrepancy in the reflectivity for the GaN logpile structures without a cavity also applies here. Since the transmission and reflectance response do not add up to 100% and GaN does not have significant absorption at these wavelengths, the observed additional loss is due to light scattering. The small discrepancy in the cavity mode wavelength position can be attributed to differences between observed PC dimensions and the nominal values used for simulations.

In conclusion, we have demonstrated nine layer logpile 3DPC structures with and without a cavity composed entirely from epitaxial single crystalline GaN fabricated using a template-directed selective MOCVD growth approach. In the future, by appropriately introducing dopants during the growth process, p−n junctions can be formed to create three-dimensional LED structures. It is worth noting here that a larger number of logpile layers could potentially be achieved by using approaches like holography[26] or laser direct write.[27] This opens up a new path to create GaN based LEDs that can utilize the PDOS enhancement offered by 3DPCs to enhance their performance. Since the 3DPC also consists of a continuous network of voids it may allow phosphors to be introduced into the volume which can be pumped by emission from the GaN. This approach would be superior to pumping phosphor coated on the surface of a planar LED since one can take advantage of the radiative enhancement of emitters offered by the 3DPC[4]. While this is an important step toward GaN based 3DPC LEDs, there are still challenges that need to be addressed such as better material quality, doping control, and most importantly issues associated with electrical contacts and current distribution before one can realize a practical device.

■ ASSOCIATED CONTENT

Supporting Information. Photoluminescence response from an unpatterned GaN reference sample region and GaN logpile three dimensional photonic crystal pumped at 266 nm. This material is available free of charge via the Internet at http://pubs.acs.org.

■ AUTHOR INFORMATION

Corresponding Author
*E-mail: gssubra@sandia.gov.

■ ACKNOWLEDGMENT

We thank Carlos Sanchez for assisting with nanofabrication. This work was performed, in part, at the Center for Integrated Nanotechnologies, a U.S. Department of Energy, Office of Basic Energy Sciences user facility. This work was performed, in part, at the Center for Integrated Nanotechnologies, a U.S. Department of Energy, Office of Basic Energy Sciences user facility. Fabrication of the PC and a portion of structural and optical characterization was performed under Sandia's Laboratory Directed Research and Development (LDRD) and a portion of structural and optical characterization and data analysis was supported by

Sandia's Solid-State-Lighting Science Energy Frontier Research Center, funded by the U.S. Department of Energy, Office of Science, Office of Basic Energy Sciences. Sandia National Laboratories is a multiprogram laboratory managed and operated by Sandia Corporation, a wholly owned subsidiary of Lockheed Martin Corporation, for the U.S. Department of Energy's National Nuclear Security Administration under contract DE-AC04-94AL85000.

REFERENCES

(1) Yablonovitch, E. *Phys. Rev. Lett.* **1987**, *58* (20), 2059.
(2) John, S. *Phys. Rev. Lett.* **1987**, *58* (23), 2486.
(3) Suzuki, T.; Yu, P. K. L. *J. Opt. Soc. Am. B* **1995**, *12* (4), 570–582.
(4) Subramania, G.; Lee, Y. J.; Fischer, A. J.; Luk, T. S.; Brinker, C. J.; Dunphy, D. *Appl. Phys. Lett.* **2009**, *95* (15), 151101–3.
(5) Aoki, K.; Guimard, D.; Nishioka, M.; Nomura, M.; Iwamoto, S.; Arakawa, Y. *Nat. Photonics* **2008**, *2* (11), 688–692.
(6) Chuang, C. M.; Lu, W. B.; Su, W. F.; Lin, C. M.; Chen, Y. F. *J. Appl. Phys.* **2005**, *97* (9), 096104–3.
(7) Lodahl, P.; Floris van Driel, A.; Nikolaev, I. S.; Irman, A.; Overgaag, K.; Vanmaekelbergh, D.; Vos, W. L. *Nature* **2004**, *430* (7000), 654–657.
(8) Wierer, J. J.; Krames, M. R.; Epler, J. E.; Gardner, N. F.; Craford, M. G.; Wendt, J. R.; Simmons, J. A.; Sigalas, M. M. *Appl. Phys. Lett.* **2004**, *84* (19), 3885–3887.
(9) Kim, J.-Y.; Kwon, M.-K.; Park, S.-J.; Kim, S. H.; Lee, K.-D. *Appl. Phys. Lett.* **2010**, *96* (25), 251103–3.
(10) Huang, C.-Y.; Ku, H.-M.; Chao, S. *Opt. Express* **2009**, *17* (26), 23702–23711.
(11) Shields, P. A.; Charlton, M.; Lee, T.; Zoorob, M. E.; Allsopp, D. W. E.; Wang, W. N. *IEEE J. Sel. Top. Quantum Electron.* **2009**, *15* (4), 1269–1274.
(12) Huang, H.; Huang, J.; Lin, C.; Lee, K.; Hsu, H.; Yu, C. *IEEE Electron Device Lett.* **2010**, *31* (6), 582–584.
(13) Lai, C. F.; Chao, C. H.; Kuo, H. C.; Yen, H. H.; Lee, C. E.; Yeh, W. Y. *Appl. Phys. Lett.* **2009**, *94* (12), 3.
(14) McGroddy, K.; David, A.; Matioli, E.; Iza, M.; Nakamura, S.; DenBaars, S.; Speck, J. S.; Weisbuch, C.; Hu, E. L. *Appl. Phys. Lett.* **2008**, *93* (10), 103502.
(15) Lee, J.; Ahn, S.; Kim, S.; Kim, D.-U.; Jeon, H.; Lee, S.-J.; Baek, J. H. *Appl. Phys. Lett.* **2009**, *94* (10), 101105.
(16) Oder, T. N.; Shakya, J.; Lin, J. Y.; Jiang, H. X. *Appl. Phys. Lett.* **2003**, *83* (6), 1231–1233.
(17) Subramania, G.; Constant, K.; Biswas, R.; Sigalas, M. M.; Ho, K. M. *Appl. Phys. Lett.* **1999**, *74* (26), 3933–3935.
(18) Wijnhoven, J. E. G. J.; Vos, W. L. *Science* **1998**, *281* (5378), 802–804.
(19) Braun, P. V.; Wiltzius, P. *Nature* **1999**, *402* (6762), 603–604.
(20) Subramania, G.; Lee, Y.-J.; Brener, I.; Luk, T. S.; Clem, P. G. *Opt. Express* **2007**, *15* (20), 13049–13057.
(21) Subramania, G.; Lee, Y.-J.; Fischer, A. J.; Koleske, D. D. *Adv. Mater.* **2010**, *22* (4), 487–491.
(22) Li, Q.; Figiel, J. J.; Wang, G. T. *Appl. Phys. Lett.* **2009**, *94* (23), 231105–3.
(23) Subramania, G.; Lee, Y.-J.; Fischer, A. J. *Adv. Mater.* **2010**, *22*, 4180.
(24) Simulations were performed using the OptiFDTD software from Optiwave assuming a material refractive index (n) of 2.5. A broad band planewave source centered at 600 nm wavelength with fwhm of 400 nm was used as the excitation source with 10 nm × 10 nm × 10 nm spatial grid with periodic and perfectly matched layer boundary conditions in the lateral directions and normal direction, respectively.
(25) The decrease (increase) in lateral lattice constant (a) which would result in a blue (red) shift of the band gap is somewhat compensated for by the red (blue) shift effect due to increase (decrease) in vertical lattice constant (c). This can be circumvented if necessary by fabricating only one lattice constant per wafer.
(26) Shir, D.; Nelson, E. C.; Chen, Y. C.; Brzezinski, A.; Liao, H.; Braun, P. V.; Wiltzius, P.; Bogart, K. H. A.; Rogers, J. A. *Appl. Phys. Lett.* **2009**, *94* (1), 011101.
(27) Wong, S.; Deubel, M.; Perez-Willard, F.; John, S.; Ozin, G. A.; Wegener, M.; von Freymann, G. *Adv. Mater.* **2006**, *18* (3), 265–269.
(28) Nelson, E. C.; Dias, N. L.; Bassett, K. P.; Dunham, S. N.; Verma, V.; Miyake, M.; Wiltzius, P.; Rogers, J. A.; Coleman, J. J.; Li, X.; Braun, P. V. *Nat. Mater.* **2011**, *10* (9), 676–681.

NOTE ADDED IN PROOF

We note that while this paper was in review we became aware of the recent work of Nelson et. al.[28] describing the epitaxial growth of three-dimensionally architectured optoelectronic devices in GaAs thus opening the exciting possibility of electrically injected operation of a 3DPC based GaN LED.